

## CEPC BOOSTER LATTICE DESIGN \*

D. Wang<sup>†</sup>, D. H. Ji, Y. M. Peng, C. H. Yu<sup>1</sup>, Y. D. Liu, Y. Zhang<sup>1</sup>, X. H. Cui, J. Y. Zhai, M. Li<sup>1</sup>,  
C. Meng, J. Gao<sup>1</sup>, Institute of High Energy Physics, Beijing, China  
<sup>1</sup>also at University of Chinese Academy of Sciences, Beijing, China

### Abstract

The CEPC booster provides electron and positron beams to the collider at different energies. The newest booster design is consistent with the TDR higher luminosity goals for four energy modes. The emittance of booster is reduced significantly in order to match the lower emittance of collider in TDR. Both FODO structure and TME structure was studied for booster design. A lot of efforts are made to overcome the difficulty of error sensitivity for the booster and hence the dynamic aperture with errors can fulfil the requirements at all energy modes. Also, the combined magnets scheme (B+S) are proposed to minimize the cost for magnets and power supplies. The design status of CEPC booster in TDR including parameters, optics and dynamic aperture is discussed in this paper.

### INTRODUCTION

CEPC booster needs to provide electron and positron beams to the collider at different energy with required injection efficiency. The injection system consists of a 30 GeV Linac, followed by a full-energy booster ring. Electron and positron beams are generated and accelerated to 30 GeV in the Linac. The beams are then accelerated to full-energy in the booster, and injected into the collider. For different beam energies of  $t\bar{t}$ , Higgs, W, and Z experiments, there will be different particle bunch structures in the collider [1]. To maximize the integrated luminosity, the injection system will operate mostly in top-up mode, and also has the ability to fill the collider from empty to full charge in a reasonable length of time [2]. The lowest field of dipole magnets in booster is 90 Gauss and the tolerance for field error at 30 GeV can be realized by the ion based magnets.

After CDR, we have reduced the emittance of collider ring and beta function at the interaction point in order to get higher luminosity for Higgs energy mode [3]. With the booster design in CDR [2, 4], it is difficult to realize the injection from booster to collider for Higgs mode even with on-axis injection scheme. For TDR design, the dynamic aperture requirement of collider ring in horizontal direction due to injection process is shown in Fig. 1. From Fig. 1, we know that the booster emittance at 120 GeV should be lower than 1.7 nm, while it is 3.6 nm in CDR.

Actually, we have made a long effort to develop a lower emittance booster since the CEPC CDR was published. After careful study and comparison among different designs, the optics based on modified-TME structure is adopted as the best candidate. The progress of booster design based on

TME structure has been published in 2021 [5]. After that, we found this design is so sensitive to errors that the dynamic aperture of booster cannot fulfil the requirement when we consider the real error effects. So the booster design with TME structure is updated to make a balance between error sensitivity and emittance. We also made an alternative booster design with FODO structure. After the comparison between FODO and TME lattice including error effects, we chose the modified-TME lattice as our baseline for TDR because only the TME can fulfil the dynamic aperture requirement at all energy modes.

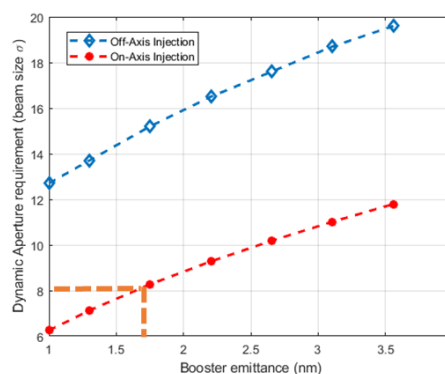


Figure 1: The dynamic aperture requirement of collider ring in horizontal direction due to injection process vs. booster emittance at 120 GeV. The horizontal emittance in collider ring at 120 GeV is 0.64 nm. The horizontal beta function at the injection point is 1800 m.

### OPTICS DESIGN FOR LOWER EMITTANCE BOOSTER

#### New Lattice Design Based on TME

The arc is made of modified-TME cells. Figure 2 shows the optics design for the arc cell. The length of TME cell in the arc is 78 m.

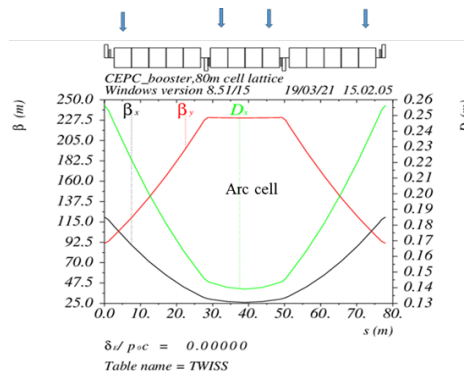


Figure 2: The Twiss functions of the TME cell in the arc region.

\* Work supported by Key Research Program of Frontier Sciences, CAS (Grant No. QYZDJ-SSW-SLH004).

<sup>†</sup> wangd93@ihep.ac.cn

The distribution for quadrupoles are arranged as uniform as possible to relax the error sensitivity of the lattice since the previous design. The horizontal phase advance is 100° and the vertical phase advance is 28° for each cell, which has been optimized carefully to make a balance between emittance and dynamic aperture. The emittance of booster at 120 GeV is reduced from 3.56 nm in CDR to 1.26 nm by this new design. The function of dispersion suppressor is to cancel the dispersion induced in the arc section and make a transition between arc section and straight section (shown in Fig. 3).

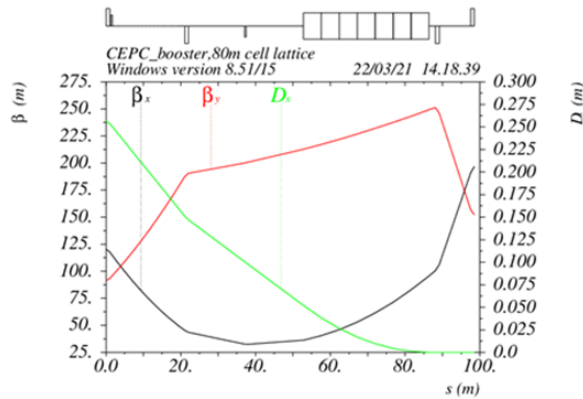


Figure 3: The Twiss functions of the dispersion suppressor.

The straight section is made of FODO cell and the length of each cell is 134 m which is shown in Fig. 4. The optimum phase advances in the arc cell and the straight FODO cell are optimized carefully in order to get the largest dynamic aperture.

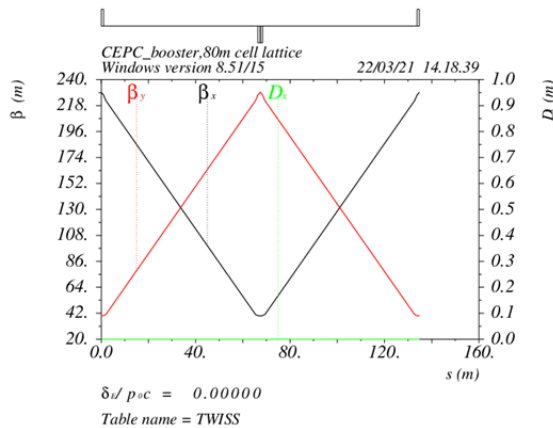


Figure 4: The Twiss functions of the FODO cell in the straight section.

### New Lattice Design based on FODO

An alternative lattice design was made based on FODO structure. This is a similar structure as CDR while the cell length is decreased to 70 m. The non-interleave sextupole scheme and 90°/90° phase advance were adopted. The emittance of FODO lattice is 1.29 nm at 120 GeV. The twiss parameters of this design are shown in Figs. 5-7.

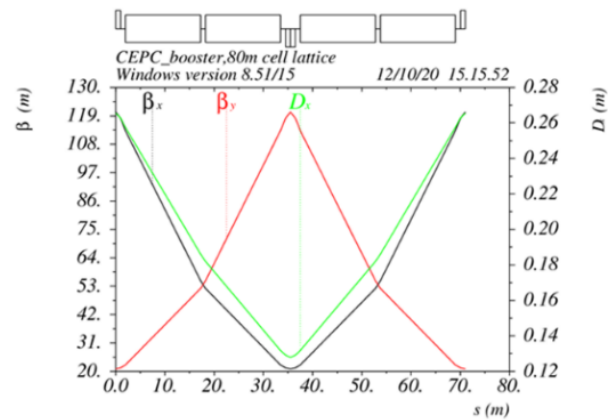


Figure 5: The Twiss functions of the FODO cell in the arc region.

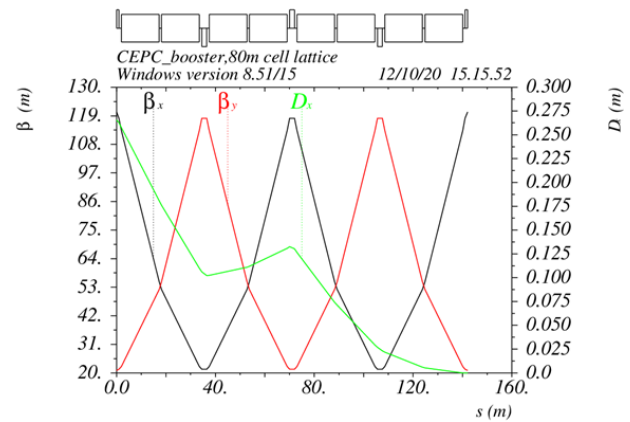


Figure 6: The Twiss functions of the dispersion suppressor.

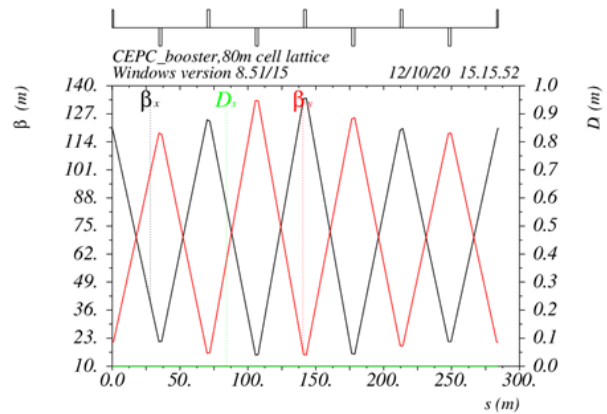


Figure 7: The Twiss functions of the straight section.

### Dynamic Aperture with Error Effects

Table 1-3 list the details of the error settings. Gaussian distribution for the errors is used and is cut off at 3  $\sigma$ . Both orbit correction (including horizontal dispersion correction) and optics correction has been done in AT. We have compared the two kinds of lattice while including the same errors, and only TME structure can meet the requirement of dynamic aperture. The DA results of TME lattice including SR effects are tracked by SAD which are shown in Figs. 8-10.

Table 1: Magnet Error Analysis Settings

Parameter	Dipole	Quad.
Transverse shift x/y (μm)	100	100
Longitudinal shift z (μm)	100	150
Tilt about x/y (mrad)	0.2	0.2
Tilt about z (mrad)	0.1	0.2
Nominal field	$1 \times 10^{-3}$	$2 \times 10^{-4}$

Table 2: BPM Analysis Settings

Parameter	BPM (10 Hz)
Accuracy (m)	$1 \times 10^{-7}$
Tilt (mrad)	10
Gain	5%
Offset after BBA(mm)	$3 \times 10^{-2}$

Table 3: Magnet Multipole Errors

Dipole	Quad.
$B1/B0 \leq 2 \times 10^{-4}$	
$B2/B0 \leq 5 \times 10^{-4}$	$B2/B1 \leq 3 \times 10^{-4}$
$B3/B0 \leq 2 \times 10^{-5}$	$B3/B1 \leq 2 \times 10^{-4}$
$B4/B0 \leq 8 \times 10^{-5}$	$B4/B1 \leq 1 \times 10^{-4}$
$B5/B0 \leq 2 \times 10^{-5}$	$B5/B1 \leq 1 \times 10^{-4}$
$B6/B0 \leq 8 \times 10^{-5}$	$B6/B1 \leq 5 \times 10^{-4}$
$B7/B0 \leq 2 \times 10^{-5}$	$B7/B1 \leq 5 \times 10^{-4}$
$B8/B0 \leq 8 \times 10^{-5}$	$B8/B1 \leq 5 \times 10^{-4}$
$B9/B0 \leq 2 \times 10^{-5}$	$B9/B1 \leq 5 \times 10^{-4}$
$B10/B0 \leq 8 \times 10^{-5}$	$B10/B1 \leq 5 \times 10^{-4}$

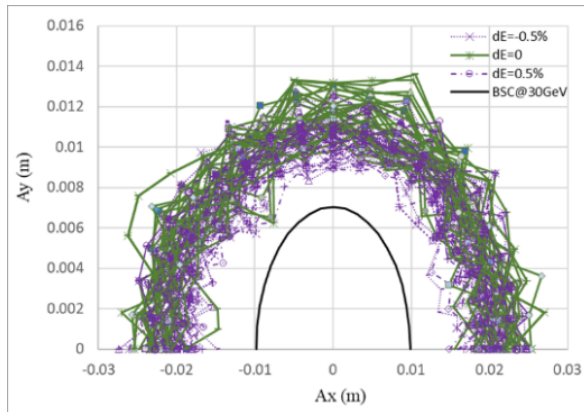


Figure 8: Dynamic aperture of booster at 30 GeV with errors and synchrotron radiation.

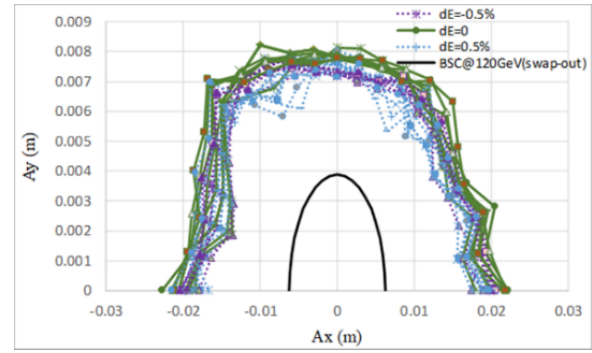


Figure 9: Dynamic aperture of booster at 120 GeV with errors and synchrotron radiation. Only the swap-out injection is considered for the BSC.

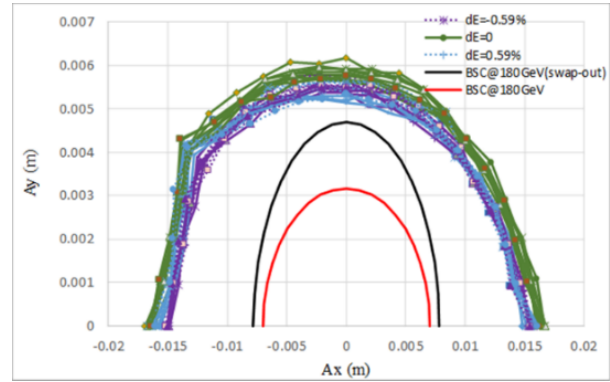


Figure 10: Dynamic aperture of booster at 180 GeV with errors and synchrotron radiation. Both the swap-out injection and off-axis injection are considered for the BSC.

## NEW PARAMETERS OF BOOSTER IN TDR

The main booster parameters at injection (30 GeV) and extraction energies are listed in Table 4 and 5. Both top up injection and full injection for CEPC can be fulfilled. For the top up injection, the assumptions are 3% current decay in collider ring, including 95% transfer efficiency for booster itself. The total beam current in the booster is less than 0.3 mA for tt running, 1 mA for Higgs mode, 4 mA for W mode and 16 mA for Z which are limited by RF system for different extraction energy. The beam is injected from linac to booster by on-axis scheme and is injected from booster to collider by off-axis scheme at three different energies for tt, W and Z. Also the on-axis injection from booster to collider has been considered at 120 GeV in case the dynamic aperture of collider ring is not large enough.

Table 4: The Main Booster Parameters at Injection Energy

		$n$	$H$	$W$	$Z$	
Beam energy	GeV	30				
Bunch number		35	268	1297	3978	5967
Threshold of single bunch current	$\mu\text{A}$	8.68	6.3	5.8		
Threshold of beam current (limited by coupled bunch instability)	$\text{mA}$	97	106	100	93	96
Bunch charge	$\text{nC}$	1.1	0.78	0.81	0.87	0.9
Single bunch current	$\mu\text{A}$	3.4	2.3	2.4	2.65	2.69
Beam current	$\text{mA}$	0.12	0.62	3.1	10.5	16.0
Growth time (coupled bunch instability)	$\text{ms}$	2530	530	100	29.1	18.7
Energy spread	%	0.025				
Synchrotron radiation loss/turn	$\text{MeV}$	6.5				
Momentum compaction factor	$10^{-5}$	1.12				
Emittance	$\text{nm}$	0.076				
Natural chromaticity	$H/V$	-372/-269				
RF voltage	$\text{MV}$	761.0	346.0	300.0		
Betatron tune $\nu_x/\nu_y$		321.23/117.18				
Longitudinal tune		0.14	0.0943	0.0879		
RF energy acceptance	%	5.7	3.8	3.6		
Damping time	$\text{s}$	3.1				
Bunch length of linac beam	$\text{mm}$	0.4				
Energy spread of linac beam	%	0.15				
Emittance of linac beam	$\text{nm}$	6.5				

Table 5: The Main Booster Parameters at Extraction Energy

		$n$	$H$		$W$	$Z$	
		Off axis injection	Off axis injection	On axis injection	Off axis injection	Off axis injection	
Beam energy	GeV	180	120		80	45.5	
Bunch number		35	268	261+7	1297	3978	5967
Maximum bunch charge	nC	0.99	0.7	20.3	0.73	0.8	0.81
Maximum single bunch current	μA	3.0	2.1	61.2	2.2	2.4	2.42
Threshold of single bunch current	μA	91.5	70		22.16	9.57	
Threshold of beam current (limited by RF system)	mA	0.3	1		4	16	
Beam current	mA	0.11	0.56	0.98	2.85	9.5	14.4
Growth time (coupled bunch instability)	ms	16611	2359	1215	297.8	49.5	31.6
Bunches per pulse of Linac		1	1		1	2	
Time for ramping up	s	7.1	4.3		2.4	1.0	
Injection duration for top-up (Both beams)	s	29.2	23.1	31.8	38.1	132.4	
Injection interval for top-up	s	65	38		155	153.5	
Current decay during injection interval		3%					
Energy spread	%	0.15	0.099		0.066	0.037	
Synchrotron radiation loss/turn	GeV	8.45	1.69		0.33	0.034	
Momentum compaction factor	10 <sup>-5</sup>	1.12					
Emittance	nm	2.83	1.26		0.56	0.19	
Natural chromaticity	H/V	-372/-269					
Betatron tune $\nu_x/\nu_y$		321.27/117.19					
RF voltage	GV	9.7	2.17		0.87	0.46	
Longitudinal tune		0.14	0.0943		0.0879	0.0879	
RF energy acceptance	%	1.78	1.59		2.6	3.4	
Damping time	ms	14.2	47.6		160.8	879	
Natural bunch length	mm	1.8	1.85		1.3	0.75	
Full injection from empty ring	h	0.1	0.14	0.16	0.27	1.8	0.8

## CONCLUSION

In the stage of TDR, a lower emittance booster has been designed in order to realize the injection for CEPC collider ring. The modified-TME structure is chosen as baseline considering all the error effects and the new design can meet the requirement for 4 energy modes. The booster parameters are updated based on the TME lattice which is consistent with CEPC TDR parameters.

## REFERENCES

- [1] D. Wang *et al.*, “Problems and considerations about the Injection philosophy and timing structure for CEPC”, *Int. J.*

*Mod. Phys. A*, vol. 37, p. 2246006, 2022.  
doi:10.1142/S0217751X2246006X

- [2] The CEPC Study Group, “CEPC conceptual design report”, Volume I- Accelerator, *Rep. IHEP-AC-2018-01*, Aug. 2018.
- [3] CEPC Study Group, “Snowmass2021 White Paper AF3-CEPC”, arXiv:2203.09451.  
doi:10.48550/arXiv.2203.09451
- [4] D. Wang *et al.*, “Design and beam dynamics of the CEPC booster”, *Int. J. Mod. Phys. A*, vol. 35, no. 15n16, p. 2041007, 2020. doi:10.1142/S0217751X20410079
- [5] D. Wang *et al.*, “Design study of CEPC lower emittance booster”, *Int. J. Mod. Phys. A*, vol. 36, no. 22, p. 2142014, 2021. doi:10.1142/S0217751X21420148